

Supporting Information

Szczepanski et al. 10.1073/pnas.1313903110

SI Materials and Methods

Experimental Design. Motion detection task. Trials for the attended condition began with a 100% valid centrally presented cue to either the right visual field (RVF) or left visual field (LVF). After a variable expectation period (3.2–9.6 s long), moving, chromatic dot patterns (100 dots moving at 7°/s in $2.8 \times 2.8^\circ$ aperture) appeared at 10.8° eccentricity from fixation in the upper visual field of the cued side. Dots moved in one of four directions, changing direction every 400 ms. We set the motion coherence of dots to 10% above each individual subject's threshold for dot motion coherence in the periphery, calculated by using a staircase procedure before scanning. The direction of the first moving dot pattern became the target motion for that block. Subjects subsequently responded, by pressing a button, when that target motion reappeared. Because the subjects needed to identify the first brief motion stimulus that appeared on the screen to identify future repeats, subjects would be unable to perform the motion detection task if they were not paying attention to this first stimulus. When the moving dots disappeared, a tone prompted subjects to covertly shift their attention back to fixation. Each trial ended with a rest period.

Trials for the unattended condition had identical timing (Fig. 1A) and visual stimulation, except there was no cue at trial onset. In the unattended condition, the motion stimuli still appeared in the periphery, but subjects ignored the stimuli and instead maintained fixation on a central cross and responded when the cross briefly changed luminance.

Pattern detection task. We presented four colorful, complex images, each a $2^\circ \times 2^\circ$ "tile," in adjacent locations, arranged as a large square, at 8–12° eccentricity from the fixation point to one of the visual field quadrants (a schematic outline of one run is shown in Fig. 2A). We presented tiles simultaneously for 250 ms, at 1 Hz, in 16-s blocks, with a temporal jitter of 250–750 ms (Fig. 2A, frames 2 and 5). We randomized the order of the tiles, their locations within the large square, and the quadrant in which tiles appeared. In the attended condition, a 500-ms, 100% valid cue (onset 1 s before tiles; frame 4) at fixation instructed subjects to covertly direct attention to one of the four peripheral locations and to count the occurrences of a target stimulus in the location closest to fixation (frame 5). Importantly, the target location was represented in gaze-centered coordinates (relative to fixation) and in object-centered coordinates (relative to the large square) that differed in field sign (e.g., when subjects directed attention to the right hemifield, the target was represented on the left side of the large square). Subjects reported the number of targets that appeared in each location at the end of each scanning run.

In the unattended condition (frame 2), the identical visual stimuli appeared in the periphery, but subjects were not cued to attend to these stimuli. Instead, subjects performed a demanding rapid serial visual presentation task at fixation, counting the number of target letters among distracters, while ignoring the peripherally presented stimuli.

We asked subjects after the scanning session what they perceived while performing the pattern detection task and they reported the perception that all four tiles were part of the same object (1).

Visual Display. We generated visual displays on a Macintosh computer (Apple Computer) by using MATLAB software (MathWorks) and Psychophysics Toolbox functions. A PowerLite 7250 liquid crystal display projector (Epson) outside the scanner room displayed the stimuli onto a translucent screen located at the end of

the scanner bore. Subjects viewed the screen at a total path length of 60 cm through a mirror attached to the head coil. The screen subtended 30° of visual angle in the horizontal dimension and 26° in the vertical dimension. A trigger pulse from the scanner synchronized the onset of stimulus presentation to the beginning of the image acquisition.

Data Analysis. Software. We analyzed data by using the AFNI software package, FreeSurfer, SUMA (<http://afni.nimh.nih.gov/afni/suma>), MATLAB, program 1dGC (<http://afni.nimh.nih.gov/sscc/gangc/1dGC>) in R (2), and FSL.

Defining ROIs. All functional images underwent a rigid motion-correction procedure to the image acquired closest in time to the anatomical scan (3). After motion correction, we geometrically unwrapped images by using a field map and magnitude image acquired in the same session (4). We smoothed data with a 4-mm Gaussian kernel and normalized each time series to its mean intensity.

We performed a multiple regression analysis for the motion and pattern detection tasks. Square-wave regressors matching the timecourse of the design were identified as regressors of interest. We convolved each regressor with a gamma-variate function to best represent the idealized hemodynamic response. For the motion detection task, attention-related activity in frontoparietal cortex was defined by contrasting the expectation period and the visually evoked activity during all attended trials with the visually evoked activity during unattended trials. We used the same contrast to define the frontoparietal attention network for the pattern detection task, except only the visually evoked activity during the attended blocks was contrasted with unattended blocks. We thresholded statistical maps at an F score of 10.80 ($P < 0.001$, uncorrected for multiple comparisons).

We defined topographic areas frontal eye field (FEF), intraparietal sulcus areas 1–5 (IPS1–IPS5) and superior parietal lobule area 1 (SPL1) in each subject ($n = 21$) by using a memory-guided saccade task: Subjects performed delayed saccades to peripheral locations arranged clockwise around a central fixation point (5, 6). We identified the voxel with the peak attention activity in each topographic area of each hemisphere and created an ROI consisting of the peak attention voxel and the six surrounding voxels in the x , y , and z directions. We identified the supplementary eye field (SEF) based on anatomical and functional characteristics (6) and created an ROI consisting of the peak attention voxel and the six surrounding voxels. We used these ROIs for the functional connectivity analyses.

For the diffusion tractography analyses, we defined bilateral masks for IPS2 and SPL1 (seed areas) and bilateral masks for FEF and SEF (target areas). We defined ROIs as voxels at the intersection between the attention activations and each topographic map or, for SEF, as all voxels activated by attention.

Eye Movement Recordings. We monitored eye movements during scanning sessions in 11 of 14 subjects performing the memory-guided saccade task, in five of eight subjects performing the motion detection task, and in all subjects performing the pattern detection task. The remaining subjects could not be eye-tracked because of technical issues at the time of the scan session. We used a stimulus screen with a hole of 1.9° in diameter located at one edge through which a subject's eye was viewed with the help of a telephoto lens (Model 504 with Long Range Optics; Applied Science Laboratories). The eye position was displayed in real time on a video monitor in the scanner control room, superimposed

on the stimulus image. The experimenter observed the eye position display to ensure that the subjects were alert and performing the appropriate task, which was to either make a saccade in the correct direction during the memory-guided saccade task or to maintain fixation throughout the motion and pattern detection tasks. We recorded eye position data on the stimulus computer through a serial interface with the eye-tracker control module. The eye tracking system, which measured the eye position at a rate of 60 Hz, had a resolution of $\sim 0.10^\circ$, and detected differences in relative eye position of $\sim 0.50^\circ$.

We used Ilab software (7) to analyze the eye movement data. For both attention tasks, we calculated separate frequency histograms of the vertical and horizontal eye position data for each subject. Data were collected and analyzed separately for periods of covert attention to each quadrant within the visual field and for periods when stimuli were presented, but subjects were not

attending peripherally. We then used two-sample *t* tests to determine whether eye movements systematically deviated in any direction during attention to any of the four quadrants. Additionally, we defined one eye movement region (EMR), $1^\circ \times 1^\circ$ in size, around the central fixation cross and calculated the number of times the gaze left this EMR. See ref. 4 for analysis details. The maximum difference in mean horizontal and vertical eye positions among the experimental conditions was 0.12 and 0.06 degrees, respectively. There were no systematic horizontal or vertical eye deviations between any of the different experimental conditions (all $P > 0.20$). Fixation was well maintained and almost never left the EMR surrounding the central fixation cross. Of the horizontal and vertical position samples, $97.6 \pm 0.5\%$ (mean, SEM) were within the EMR during a given scan session. This analysis confirms that subjects maintained fixation throughout trials/blocks and did not shift their gaze location along with attention.

1. Blake R, Lee SH (2005) The role of temporal structure in human vision. *Behav Cogn Neurosci Rev* 4(1):21–42.
2. Pfaff B (2008) VAR, SVAR and SVEC models: Implementation within R package vars. *J Stat Softw* 27(4):1–32.
3. Cox RW, Jesmanowicz A (1999) Real-time 3D image registration for functional MRI. *Magn Reson Med* 42(6):1014–1018.
4. Jezzard P, Balaban RS (1995) Correction for geometric distortion in echo planar images from B0 field variations. *Magn Reson Med* 34(1):65–73.
5. Sereno MI, Pitzalis S, Martinez A (2001) Mapping of contralateral space in retinotopic coordinates by a parietal cortical area in humans. *Science* 294(5545):1350–1354.
6. Szczepanski SM, Konen CS, Kastner S (2010) Mechanisms of spatial attention control in frontal and parietal cortex. *J Neurosci* 30(1):148–160.
7. Gitelman DR (2002) ILAB: a program for postexperimental eye movement analysis. *Behav Res Methods Instrum Comput* 34(4):605–612.

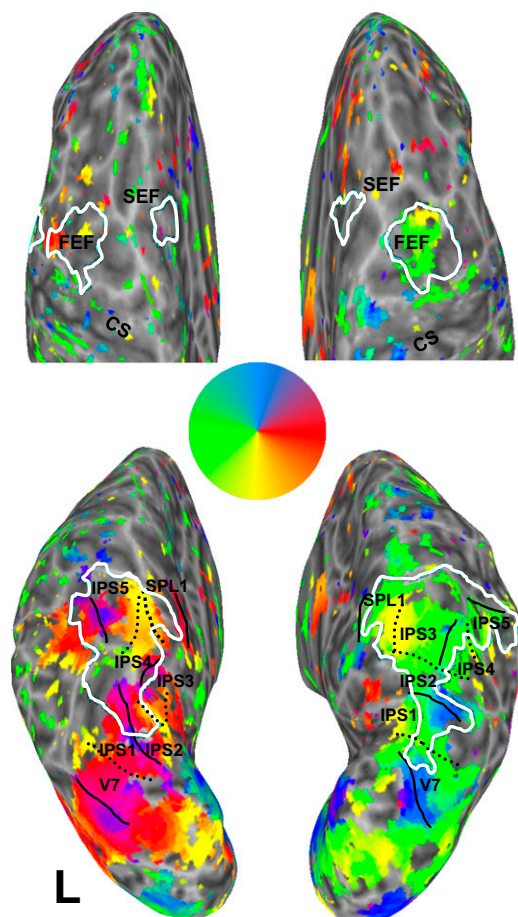


Fig. S1. Posterior parietal cortex (PPC) areas and FEF show topographic organization, whereas SEF does not. Topographic maps in frontal (*Upper*) and parietal (*Lower*) cortex from a representative subject, obtained using the memory-guided saccade task and projected onto an inflated surface of the subject's brain. The color legend represents the saccade direction/memorized location to which voxels most respond. Boundaries between PPC areas are marked by black lines, with continuous lines denoting the upper vertical meridian, and broken lines denoting the lower vertical meridian. White lines define the extent of the attention activations (attended vs. unattended, $P < 0.001$) in the same subject while performing the motion detection task. IPS1–5, SPL1, and FEF showed topographic organization and also contained attention-activated voxels. There was no evidence of topographic organization in the SEF, even when activity from the memory-guided saccade task was set to a liberal threshold (as shown), but the SEF was still significantly activated by the motion detection task. CS, central sulcus.

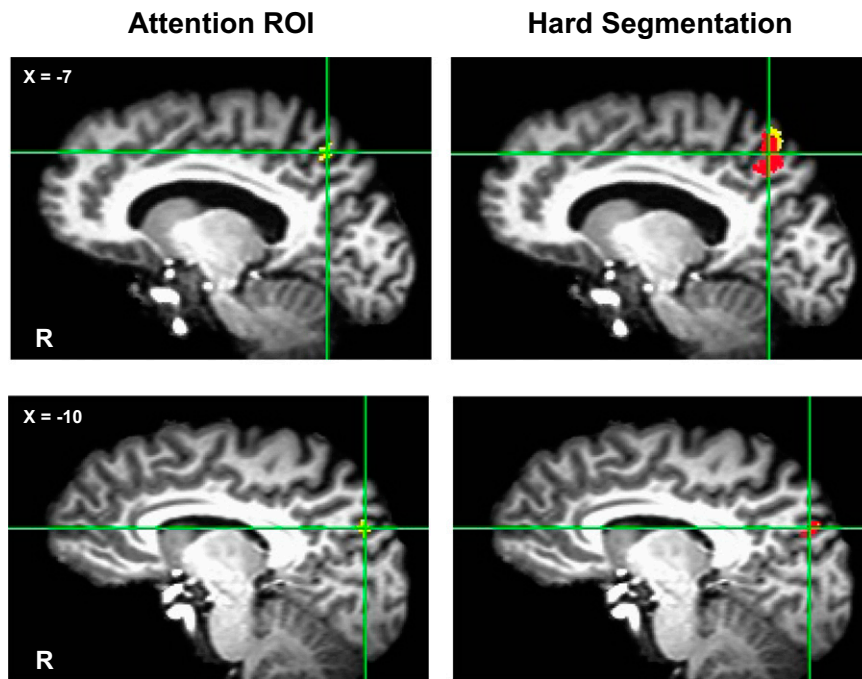


Fig. S3. Overlap between SPL1 voxels functionally connected with SEF and SPL1 voxels structurally connected to SEF. (*Left*) Peak attention ROIs (yellow voxels) in SPL1 of two example subjects (*Upper* and *Lower*). (*Right*) Corresponding hard segmentation of SPL1 in the same subjects. Red voxels in SPL1 project to the SEF, whereas yellow voxels project to the FEF.